



**HAL**  
open science

## Characterization of copper-containing porphyrins in an insoluble fraction of a bio-crude obtained from hydrothermal liquefaction of wild microalgae

Julien F. Maillard, Charlotte Mase, Olivier Serve, Herve Vezin, Carlos Afonso, Pierre Giusti, Caroline Mangote

### ► To cite this version:

Julien F. Maillard, Charlotte Mase, Olivier Serve, Herve Vezin, Carlos Afonso, et al.. Characterization of copper-containing porphyrins in an insoluble fraction of a bio-crude obtained from hydrothermal liquefaction of wild microalgae. *Algal Research*, 2023, *Algal Research*, 73, pp.103166. 10.1016/j.algal.2023.103166 . hal-04138881

**HAL Id: hal-04138881**

**<https://hal.univ-lille.fr/hal-04138881>**

Submitted on 23 Jun 2023

**HAL** is a multi-disciplinary open access archive for the deposit and dissemination of scientific research documents, whether they are published or not. The documents may come from teaching and research institutions in France or abroad, or from public or private research centers.

L'archive ouverte pluridisciplinaire **HAL**, est destinée au dépôt et à la diffusion de documents scientifiques de niveau recherche, publiés ou non, émanant des établissements d'enseignement et de recherche français ou étrangers, des laboratoires publics ou privés.

## Journal Pre-proof

Characterization of copper-containing porphyrins in an insoluble fraction of a bio-crude obtained from hydrothermal liquefaction of wild microalgae

Julien F. Maillard, Charlotte Mase, Olivier Serve, Hervé Vezin, Carlos Afonso, Pierre Giusti, Caroline Mangote



PII: S2211-9264(23)00199-6

DOI: <https://doi.org/10.1016/j.algal.2023.103166>

Reference: ALGAL 103166

To appear in: *Algal Research*

Received date: 1 December 2022

Revised date: 17 January 2023

Accepted date: 31 May 2023

Please cite this article as: J.F. Maillard, C. Mase, O. Serve, et al., Characterization of copper-containing porphyrins in an insoluble fraction of a bio-crude obtained from hydrothermal liquefaction of wild microalgae, *Algal Research* (2023), <https://doi.org/10.1016/j.algal.2023.103166>

This is a PDF file of an article that has undergone enhancements after acceptance, such as the addition of a cover page and metadata, and formatting for readability, but it is not yet the definitive version of record. This version will undergo additional copyediting, typesetting and review before it is published in its final form, but we are providing this version to give early visibility of the article. Please note that, during the production process, errors may be discovered which could affect the content, and all legal disclaimers that apply to the journal pertain.

© 2023 Published by Elsevier B.V.

# Characterization of copper-containing porphyrins in an insoluble fraction of a bio-crude obtained from hydrothermal liquefaction of wild microalgae

Julien F. Maillard<sup>1,2</sup>, Charlotte Mase<sup>1,2,4</sup>, Olivier Serve<sup>4</sup>, Hervé Vezin<sup>3</sup>, Carlos Afonso<sup>1,2\*</sup>, Pierre Giusti<sup>1,2,4</sup> and Caroline Mangote<sup>2,4</sup>

<sup>1</sup>Normandie Université, COBRA, UMR 6014, FR 3038, Université de Rouen, INSA de Rouen-Normandie, CNRS, IRCOF, Mont Saint Aignan Cedex.

<sup>2</sup>International Joint Laboratory - iC2MC: Complex Matrices Molecular Characterization, TRTG, BP 27, 76700 Harfleur, France.

<sup>3</sup>Univ.Lille Laboratoire de Spectroscopie pour les Interactions, la Réactivité & l'Environnement (LASIRE) – UMR CNRS 8516, Université de Lille, F-59000 Lille, France

<sup>4</sup>TotalEnergies OneTech, TotalEnergies Research & Technology Gonfreville, BP 27, 76700 Harfleur, France.

Corresponding author:

University of Rouen

UMR 6014 COBRA / IRCOF

Rue Lucien Tesnière

76130 Mont Saint Aignan

France

+33 2 35 52 29 40

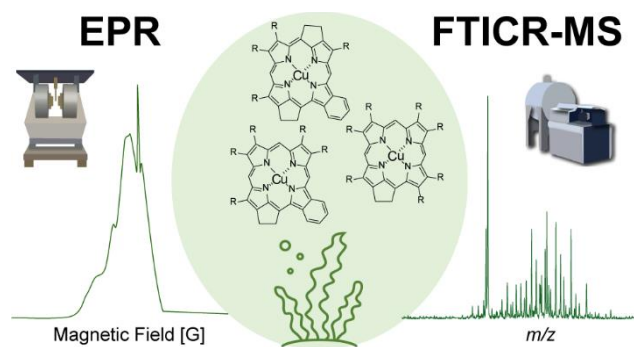
carlos.afonso@univ-rouen.fr

**Abstract**

Among the various alternatives to fossil energies, microalga-based fuels are promising solutions. Thanks to their ability to grow under harsh conditions and trap industrial exhaust gases, these microalgae can help reduce global warming effects. One efficient way to process this feedstock is to use hydrothermal liquefaction (HTL) which leads to an intermediate bio-crude and a residual solid. This bio-crude can be further refined to produce usable biofuel by eliminating problematic heteroatoms such as nitrogen, oxygen, and metals. The residual solid, which can represent 50% in mass is, however not useable nowadays. To valorize this insoluble fraction, the present work is focused on its molecular characterization and, in particular, on its metal content. Metals are particularly problematic for downstream processes when they are in an organic form such as porphyrins as they destroy catalysts. Identification and speciation of these metal organic species is thus needed. However, these analyses are challenging because of the high molecular diversity of these samples. Here, complementarity between electron paramagnetic resonance spectroscopy (EPR) and FTICR-MS, which is a state-of-the-art mass spectrometer was used for the speciation of copper elements in the residual solid. A signal characteristic of a copper surrounded by four symmetric nitrogen atoms was observed in EPR, suggesting porphyrinic structures. The dynamic range of FTICR-MS broadband analyses was not sufficient to access the isotopic fine structure of the copper porphyrins. Continuous accumulation of selected ions analyses (CASI) was thus, performed to boost the dynamic range of the mass spectrometer in a narrower mass range allowed to confirm for the first time the presence of copper porphyrins in a residual solid of bio-crude. Different families of copper porphyrins were observed, and putative structures were proposed.

Keywords: EPR, FTICR-MS, copper porphyrins, algae, hydrothermal liquefaction

Graphical Abstract:



Journal Pre-proof

## 1. Introduction

The acceleration of global warming has prompted the scientific community to seek sustainable energy solutions. One major challenge is the reduction of greenhouse gases produced by the consumption of fossil fuels. Among the different alternatives, microalga-based fuels are promising solutions. Due to their fast growth rate, cultivation on non-arable lands, and potential high lipid content microalgae are of particular interest. In recent projects, wild microalgae were fed using exhaust gases of industries, allowing the capture of CO<sub>2</sub> [1-3]. One way to process harvested microalgae mixtures is to use hydrothermal liquefaction (HTL). HTL has been reported as an efficient way to process such feedstock in numerous published reviews [4-8]. Using a direct thermochemical conversion of wet microalgae, this process avoids preliminary energy-consuming drying steps. Moreover, the temperature and pressure process conditions allow to exploit the specific water properties for the bio-molecules conversion through hydrolysis, decarboxylation and dehydration. Obtained products are the bio-crude (a liquid), some gases, and a solid residue resulting from heavy fragments and molecule condensations. The obtained bio-crude is the only valorized product nowadays. However, it was reported in a previous work that the amount of solid residue can reach 50 % in mass [3]. Finding ways to valorize this fraction is thus, important. To this end, understanding its molecular composition is an important preliminary step. However, this residue is composed of thousands of different species which makes it challenging to study. Inductively coupled plasma atomic emission spectrometry (ICP-AES) after mineralization conducted on these samples has revealed the presence of several metals and especially iron and copper [3]. Such metals can be present either in a form of salt or in organic forms including porphyrins. This metal-organic form is particularly problematic during downstream processes as it destroys catalysts. Iron porphyrins were already identified and characterized in this kind of bio-crudes in previous works using Fourier transform ion cyclotron resonance

mass spectrometry (FTICR-MS) [9, 10]. FTICR-MS are state-of-the-art instruments that deliver very high performances in terms of resolution, mass accuracy, and the dynamic range, which is required to resolve the highly complex samples and attribute to each detected signal a unique molecular formula [11-13]. However, additional metals are contained into this residue, but no organic signatures were detected with these analyses. Indeed, only a limited number of elements are considered for molecular formula assignments such as carbon, hydrogen, nitrogen, oxygen and sulfur [14]. The consideration of additional elements will yield necessary to an increase of wrong attributions so this should be performed carefully and typically with additional knowledge of the sample for instance based on ICP-MS analysis [15, 16]. Electron paramagnetic resonance (EPR) spectroscopy measures the resonant absorption of microwave radiation in the presence of a static magnetic field [17, 18]. Absorptions are observed when the spin or the orbital angular momentum of an unpaired electron creates a magnetic dipole [17]. This technique is particularly useful for the characterization of metals-containing species [19]. It has proved its usefulness for the characterization of vanadyl porphyrins in asphaltenes from the Athabasca oils sands [20]. In this work, EPR measurements were performed to observe behavior of copper. Signal of a copper surrounded by four nitrogen atoms was observed, assuming a porphyrinic structure. FTICR-MS measurements using continuous accumulation of selected ions (CASI) [21] was then conducted to identify the structure of this organic copper.

## 2. Experimental part

### 2.1. Production of the bio-oil

The production of the bio-oil is described in a previous paper [3]. Briefly, cultivation of algae took place in an industrial environment using CO<sub>2</sub> from plant emission without any purification as carbon sources. In this context, the cultivated algae were wild algae as ambient indigenous species as opposed to inoculated selected species. After the harvesting procedure, hydrothermal liquefaction conversion (HTL) was performed to transform algae into a bio-crude. This bio-crude was characterized in a previous work [3]. It was, then, further refined using distillation to remove the water and liquid/solid extract on with hot toluene. Obtained products were bio-oil and a solid residue with a proportion of 50% for each. Elemental composition of the bio-crude is given in table S1 and the insoluble fraction elemental content in table S2. In the present work, we focused our effort on the solid fraction of a bio-crude from algae produced in fresh water during winter 2018.

### 2.2. Solid-state EPR spectroscopy

Echo field sweep and 2D hyperfine sublevel correlation (HYSCORE) spectra were recorded with a Bruker ELEXYS E580 spectrometer (Bruker, Bremen, Germany) operating at a temperature  $T = 5\text{K}$  using a CoolEdge cryofree system [22]. For pulsed 2D HYSCORE experiments, a four-pulse sequence  $(\pi/2)-\tau-(\pi/2)-t_1-(\pi)-t_2-(\pi/2)-\text{detection}(\text{echo})$  sequence was used with pulse lengths of  $\pi/2$  and  $\pi$  pulses of 16 ns and 32 ns and a delay  $\tau = 136$  ns for  $+1/2$  copper excitation line and pulses lengths of  $\pi/2$  and  $\pi$  pulses of 28 ns and 56 ns and the delay  $\tau = 136$  ns for selective excitation of carbon-centered radical species. The 2D spectra were acquired with  $256 \times 256$  time-domain data points to build  $t_1$  and  $t_2$  dimensions. The unmodulated part of the echo was removed by second-order polynomial subtraction. Finally,



2D Fourier transformation and a Hamming apodization window function were applied to obtain the 2D HYSCORE spectra.

### **2.3.FTICR-MS**

All analyses were performed on an FTICR Solarix XR (Bruker Daltonics, Bremen, Germany) equipped with a 12 T superconducting magnet and a laser desorption ionization (LDI) source used in positive ion mode. The mass spectrometer was externally calibrated with a solution of sodium trifluoroacetate. Mass spectra were afterward internally calibrated with confidently assigned signals yielding a mass accuracy below 300 ppb in the considered mass range. A sample of the insoluble fraction of the bio-crude was deposited using a solvent-free method, following a previously published procedure [23]. Mass spectra were recorded in positive ion mode at 8 million points with a sum of 500 scans, yielding a resolution of 1 500 000 at  $m/z$  150 and 500 000 at  $m/z$  500. The following instrumental parameters were implemented: Plate offset at 100 V, deflector plate at 210 V, laser power at 19 %, number of laser shots at 40, frequency of laser shots at 1000 Hz, funnel 1 at 150 V, skimmer 1 at 25 V. To boost the dynamic range of the FTICR-MS and achieve better sensitivity for low-abundance species, continuous accumulation of selected ions (CASI) experiments were conducted [21]. For this purpose, the porphyrinic region (between  $m/z$  425 and  $m/z$  675) was isolated thanks to the quadrupole and then transferred to the infinity ICR cell. Data acquisition and data treatment were performed using FTMS Control (version 2.3, Bruker Daltonics, Bremen, Germany) and DataAnalysis (version 5.1, Bruker Daltonics, Bremen, Germany) respectively.

### 3. Results and discussion

#### 3.1. EPR results

The insoluble fraction was analyzed by pulse EPR techniques at 5 K. The low temperature is used to decrease the number of spins at the high energy level. The spectrum displayed in Figure 1 shows the echo field sweep spectrum representing the echo intensity corresponding to the first derivative of the imaginary part of the molecular magnetic susceptibility concerning the external static magnetic field (in arbitrary unit) in the function of magnetic field (in gauss). We can see a typical  $\text{Cu}^{2+}$  (d9 electronic spin  $S=1/2$ ) species with a g value of 2.11. The g factor is a constant of proportionality, whose value is the property of the electron in a particular environment. It was calculated thanks to Equation 1 with  $\nu$  the X-band microwave frequency in GHz and B the magnetic field in mT. Note that one tesla corresponds to 10000 gauss.

$$\text{Equation 1. } g = 71.4484 \nu / B$$

It presented also a hyperfine interaction with  $^{63}\text{Cu}$  (nuclear spin  $I=3/2$ ) with a coupling constant of  $A = 212$  G. This interaction corresponded to a local magnetic field induced by unpaired electrons of the compound. This interaction allowed us to provide crucial information about the sample such as the number and the identity of atoms in a molecule or compound, as well as their distance from the unpaired electron. In our case and according to Peisach-Blumberg [24], the obtained hyperfine interaction indicates a four nitrogen atoms coordination around the  $\text{Cu}^{2+}$ . Moreover, superhyperfine coupling was also observed and corresponded to additional smaller splitting from nearby nuclei. This superhyperfine coupling was observed in the  $+1/2$  copper hyperfine transition with a pattern of nine lines resulting from the superhyperfine coupling of  $\text{Cu}^{2+}$  electron spin with 4 equivalent nitrogen atoms ( $I=1$ ) with the superhyperfine coupling of 17 G. Such results are typical of copper porphyrin structure.

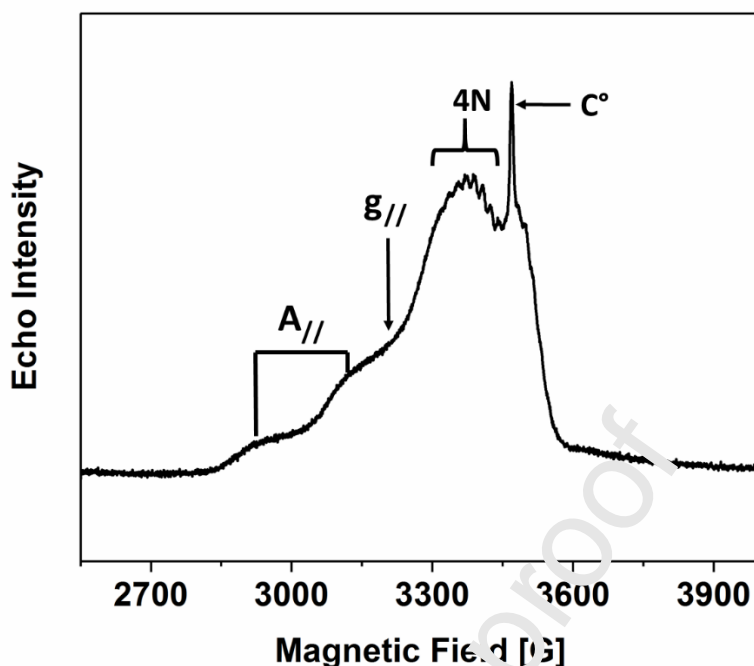


Figure 1. Echo field sweep spectrum of insoluble fraction recorded at 5 K

To go further insight into the environment and have access to the local structure of copper porphyrin and carbon-centered radical, 2D-HYSCORE experiments have been performed. Such experiments allow transferring electron magnetization to surrounding nuclei by mixing the two electron spin manifolds. Figures 2a and 2b display the results for copper moiety and radical species respectively. Peaks appearing in the upper right (+, +) quadrants typically arise from nuclei in which the hyperfine coupling is less than the Larmor frequency. They appear at the Larmor frequency, separated by the hyperfine coupling. Peaks from nuclei in which the hyperfine interaction is greater than the Larmor frequency appear in the upper left (-, +). For the copper species (Figure 2a) only weak coupling with  $^{13}\text{C}$  and  $^1\text{H}$  in the (+, +) quadrant is observed with respectively hyperfine constant  $A_{\text{iso}}$  of 5.8 MHz and 2.1 MHz. This weak coupling results from the second sphere coordination of the porphyrin. No nitrogen atoms couplings are observed. Effectively echo field sweep experiment shows a coupling of 17G (~ 48 MHz) with nitrogen that is too high compared to the bandwidth to be observed, i.e. 20

MHz. For the carbon-centered radical (Figure 2b), a nitrogen atom pattern that contributes to both quadrants can be observed. In the (+, +) quadrant we can observe a  $^{14}\text{N}$  pattern at 4.6 MHz that can be assigned to the double quantum (dq). In the (-, +) quadrant single quantum (sq) and dq for  $^{14}\text{N}$  can be measured. Two dq peaks with  $A_{\text{iso}}$  of 6.1 and 7.8 MHz indicate that two different nitrogen atoms are inserted in this radical structure. Weak coupling in the (+, +) quadrant for  $^{13}\text{C}$  and  $^1\text{H}$  is also observed with a maximum value of 10 MHz for protons.

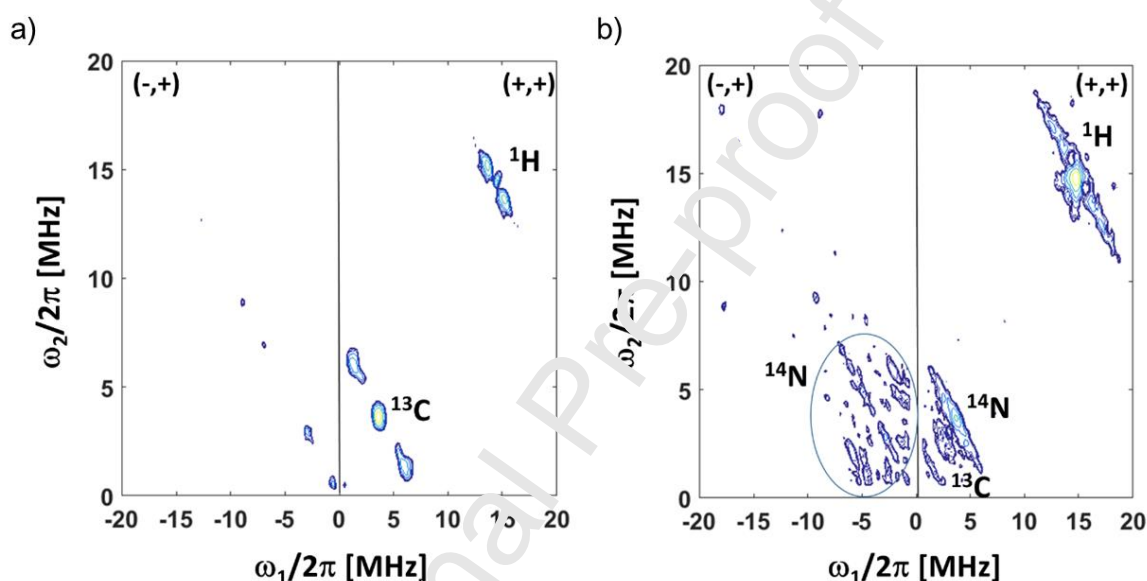


Figure 2: 2D-HYSCORE spectra of (a) copper (+1/2 line) species and (b) carbon-centered radical. Spectra were recorded at 5 K

## 2.2. FTICR results

To obtain a molecular characterization of suspected copper porphyrins, Laser Desorption Ionization coupled to Fourier transform ion cyclotron resonance mass spectrometry (LDI-FTICR-MS) was used. LDI has proven to be particularly efficient for the ionization of porphyrins and has the advantage to work with either liquid or solid samples [23, 25-28]. A FTICR mass spectrometer was used for this analysis, allowing the best performances in terms of resolution, mass accuracy, and dynamic range.[12, 29-31] Initial broadband LDI-FTICR

experiment yielded to the detection of signals consistent with copper-containing species. However, the signal-to-noise was not sufficient to detect  $^{65}\text{Cu}$  isotopes (Figure S1). To improve the dynamic range and facilitate the observation of  $^{65}\text{Cu}$  isotopes, continuous accumulation of selected ions (CASI) was performed on the porphyrin signals region (between  $m/z$  425 and  $m/z$  675) [32]. CASI involved to the use of the quadrupole mass filter to transmit a small proportion of the ions to the ICR cell. The number of ions that are introduced to the ICR cell is controlled by the accumulation time (typically in the ms range). It is limited by charge space effects that can yield to change in ion frequency and even to coalescence effect [33]. With CASI a higher amount of ions of this narrower mass range is trapped in the ICR cell using a higher accumulation time. As a consequence, this greatly enhances the dynamic range of the analysis. A better sensitivity for low-abundance species was therefore obtained.

Obtained results are reported in Figure 3. Figure 3a presents the acquired mass spectrum with the broadband mass spectrum colored in black and the CASI experiment is in red. The first observation that can be enounced is the very high number of signals obtained in the analyzed insoluble fraction of the bio oil. Figure 3b presents a zoom at  $m/z$  537 on 400 mDa. This zoom highlights the complexity of the sample with more than 50 signals detected in this range. The mass accuracy and the resolution of the FTICR however allow the molecular formula attribution of each detected signal. Several molecular formulas are also reported in the inset. It can also be observed around  $m/z$  450 the presence of intense signals that spike out of the distribution. These signals correspond to iron porphyrins [34, 35].

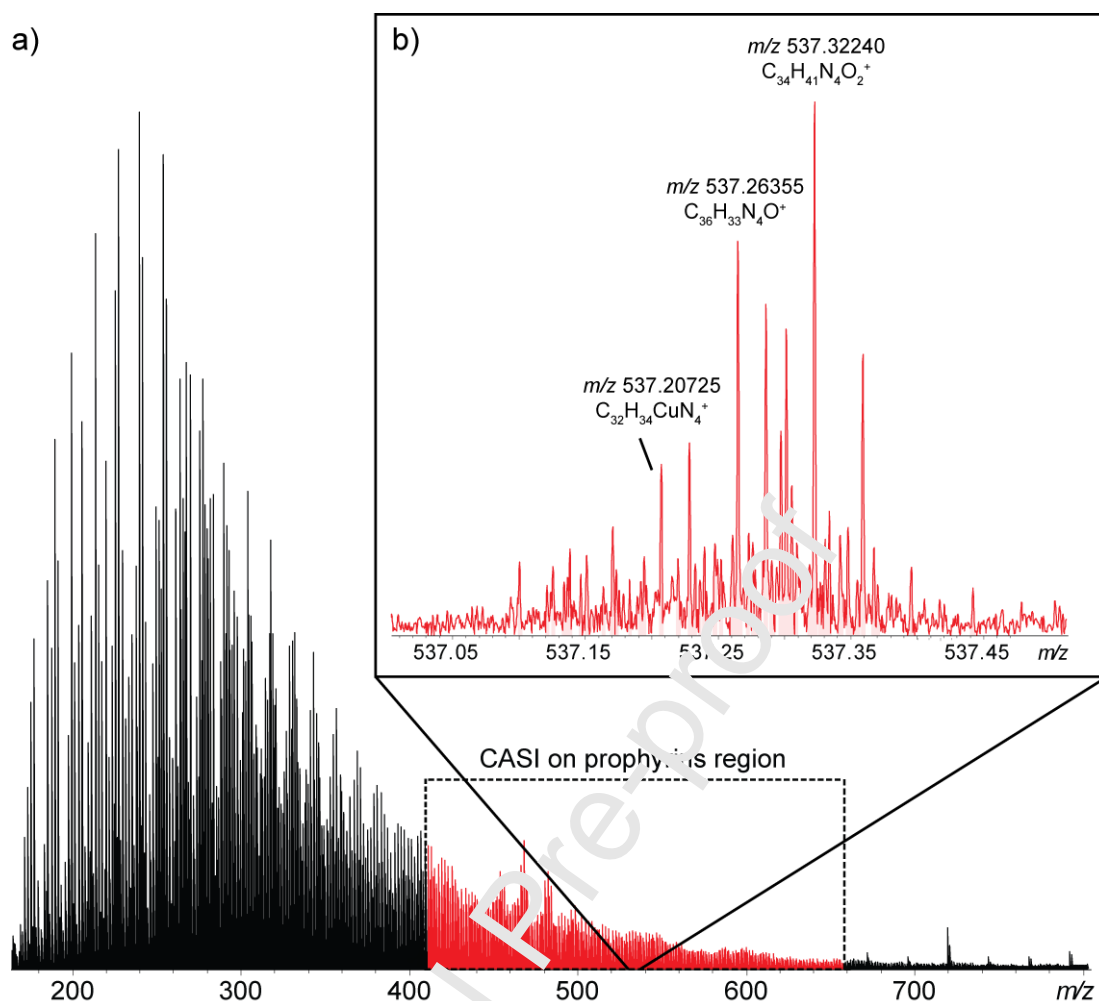


Figure 3. Obtained broadband (in black) and CASI isolation (in red) mass spectra of the insoluble fraction of the bio-crude analyzed by LDI-FTICR-MS in positive ion mode. The inset presents a nominal mass zoom at  $m/z$  537. Several species were attributed and added to this inset.

To research specifically suspected copper porphyrins, the constraints applied to the molecular formula attribution algorithm were as followed:  $N_4Cu_1O_0$  and a minimal double bond equivalent (DBE) value of 17 according to the minimal possible core (tetrapyrrole). Even with the high mass accuracy of the FTICR, several molecular formulas were found for the same signal and isotopic fine structure verification was needed to find real copper porphyrins. Figure 4 presents an example of the CASI mass spectrum between  $m/z$  537 and  $m/z$  541 of the insoluble fraction of the bio-crude (in red) with the simulated isotopic pattern of the molecular formula  $C_{32}H_{34}N_4Cu^+$  suspected as a good candidate for the detected signal at  $m/z$  537.20740 (in black). The mass deviation is 50 ppb compared to the calculated mass. This experimental

mass is also consistent with the  $C_{38}H_{25}N_4^+$  molecular formula one with a deviation of only 10 ppb. Its simulated pattern is colored in blue. Zooms at  $m/z$  537 and  $m/z$  539 were given in Figures 4b and 4c respectively to compare the experimental measurement and the simulated isotopic pattern.

By comparing the simulated isotopic pattern with the experimental measurement, it was found at  $m/z$  539 (monoisotopic signal at +2 Da compared to most abundant Cu isotope of  $C_{32}H_{34}N_4Cu^+$ ) a signal corresponding to the molecular formula  $C_{32}H_{34}N_4^{65}Cu^+$ . Molecular attribution of this signal provided no other possibility. In contrast, the signal of the  $C_{36}H_{25}N_4^{13}C_2^+$  ion is not present in Figure 4c. As a consequence, the detection of such the  $^{65}Cu$  isotope validates the molecular formula of the copper porphyrin  $C_{32}H_{34}N_4Cu^+$ .

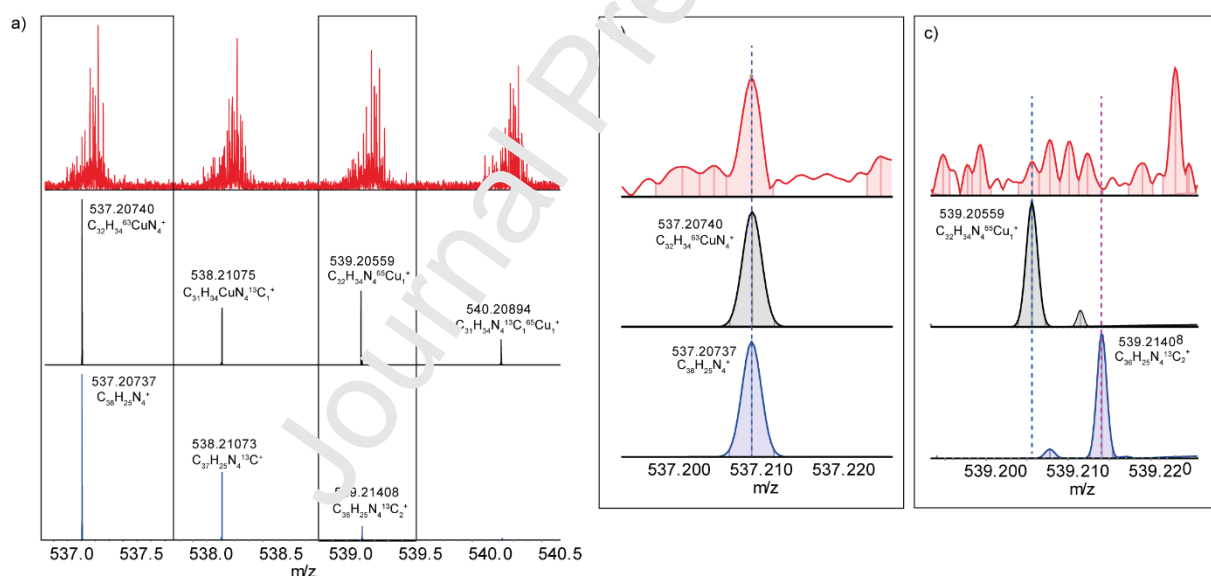


Figure 4. CASI LDI-FTICR-MS mass spectrum showing (a) the  $m/z$  537-540 range of the insoluble fraction of the bio-crude (in red), a simulated isotopic pattern of the molecular formula  $C_{32}H_{34}CuN_4^+$  (in black), and a simulated isotopic pattern of the molecular formula  $C_{38}H_{25}N_4^+$  (in blue). Additional zooms at (b) monoisotopic ion and (c) at monoisotopic +2 Da were also given.

The signal of copper porphyrin detected at  $m/z$  537.20740 was the most intense at present already a relative intense  $^{65}Cu$  isotope. For lower intensity copper porphyrin signals, the

detection of  $^{65}\text{Cu}$  is not always possible. One strategy to assign unambiguously additional copper porphyrins is to take advantage of the negative mass defect of copper ( $M_{\text{Cu}}$ : 62.92960 u,  $MD_{\text{Cu}} - 0.07040$  u) by the use of Kendrick mass defect (KMD) plots [36, 37]. Kendrick mass defect is defined by Equation 2.

$$\text{Equation 2. } KMD = \text{Observed nominal mass} - \text{Observed mass} \times \frac{14}{14.01565}$$

The KMD allows taking out the mass defect contribution of the  $\text{CH}_2$  repetition unit from a measured  $m/z$ . By representing this KMD *versus* the Kendrick nominal mass it is possible to generate two-dimensional plots of the mass spectrum, where the  $x$ -axis is the nominal mass of the  $m/z$  value and the  $y$ -axis is the decimal one. Species of the same family which only differ by the number and length of alkyl groups (number of  $\text{CH}_2$  repetition units) are on the exact same  $y$ -axis and have therefore the same KMD value. The obtained plot was made using a Python script PyC2MC viewer [38] and is given in Figure 5a. Here, the black dots represent all signals peak picked in the mass spectrum. In Figure 5b, the previously detected copper porphyrin with a molecular formula of  $\text{C}_{32}\text{H}_{34}\text{N}_4\text{Cu}^+$  was added using a pink star. Then, by adding or subtracting exactly the mass of  $\text{CH}_2$  to the starting porphyrin ( $\text{C}_{32}\text{H}_{34}\text{N}_4\text{Cu}^+$ ) with a tight error interval ( $14.01565 \pm 0.0005$  Da), other copper porphyrins of the analysis could be identified. The same procedure was applied with the addition and subtraction of the mass of  $\text{H}_2$  to detect copper porphyrins having a different DBE value. In this range of 0.5 mDa, only signals having exactly the correct value are recovered, allowing a very precise attribution pathway. The resulting identified series are presented in Figures 5a and 5b. It can be observed



that copper porphyrins are detected with a DBE varying from 17 to 23 with different number and lengths of alkyl chains. Examples of attributed molecular formulas are given in Table 1 and an exhaustive list is given in supporting information in Table S3.

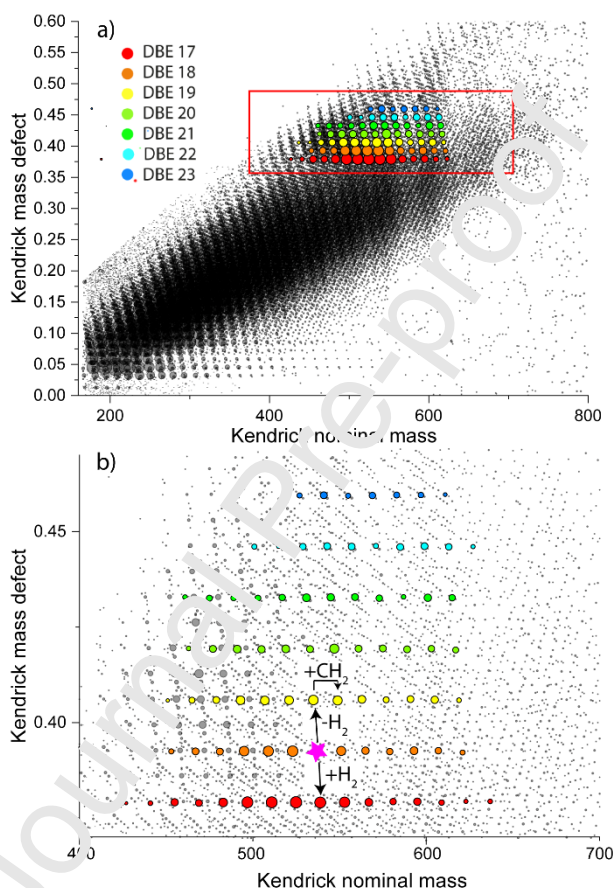


Figure 5. Kendrick mass defect *versus* Kendrick nominal mass diagram of (a) the whole  $m/z$  peak list of the analyzed bio-crude (black) and the extracted copper porphyrins (from red to blue) for each value of DBE and (b) zoom of porphyrin region.

**Table 1:** Example of attributed molecular formula of copper porphyrins

Intensity (arbitrary unit)	Calc. $m/z$	Err (ppm)	Molecular formula	DBE
2746443	441.113496	-0.072	$C_{25}H_{22}CuN_4$	17
5757098	469.144796	-0.001	$C_{27}H_{26}CuN_4$	17
1467602	425.082196	-0.012	$C_{24}H_{18}CuN_4$	18
2754068	453.113496	0.011	$C_{26}H_{22}CuN_4$	18

1130983	423.066546	0.175	$C_{24}H_{16}CuN_4$	19
2036204	451.097846	0.214	$C_{26}H_{20}CuN_4$	19
3310538	477.113496	0.051	$C_{28}H_{22}CuN_4$	20
5040052	491.129146	0.006	$C_{29}H_{24}CuN_4$	20
1061847	433.050896	0.137	$C_{25}H_{14}CuN_4$	21
1215822	447.066546	-0.189	$C_{26}H_{16}CuN_4$	21
1550163	459.066546	-0.063	$C_{27}H_{16}CuN_4$	22
1827498	473.082196	0.092	$C_{28}H_{18}CuN_4$	22
4529688	541.144796	0.080	$C_{33}H_{26}CuN_4$	23
5751931	555.160446	0.112	$C_{34}H_{28}CuN_4$	23

Using obtained molecular formulas of copper porphyrins, several putative structures were drawn and are given in Figure 6. Such structures are based on previous research on vanadium petroporphyrins [13, 25, 39, 40].

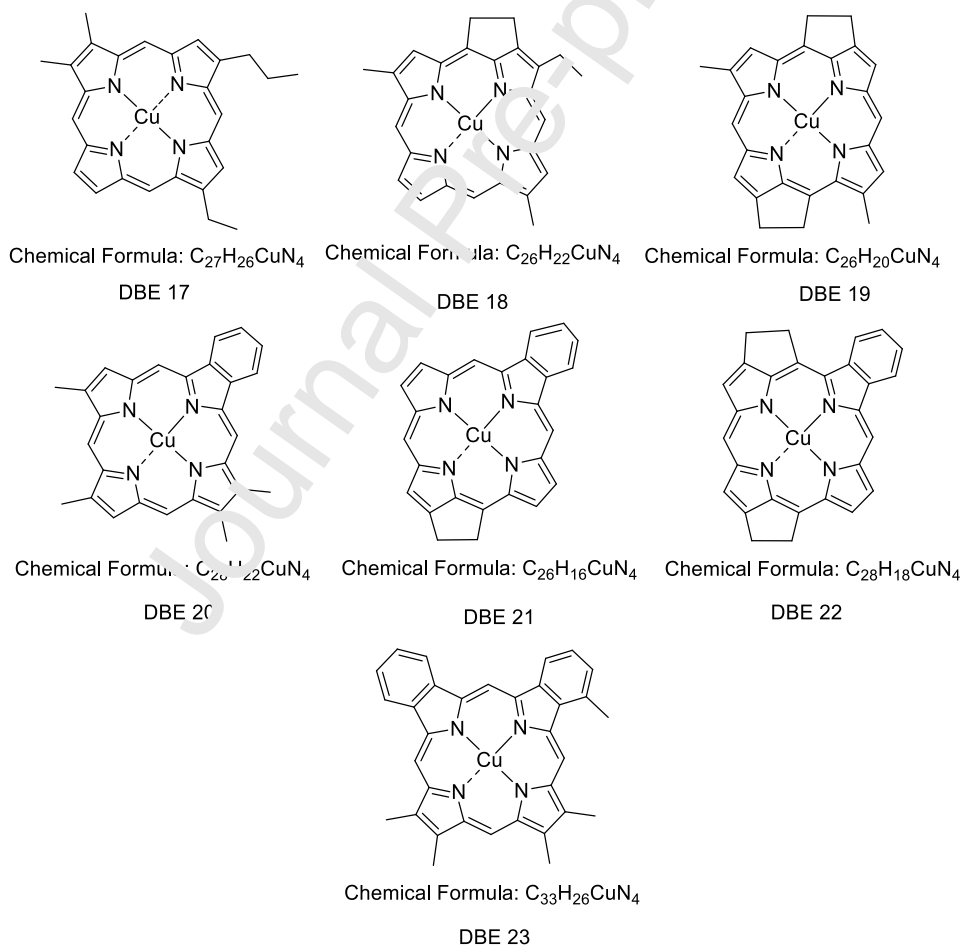


Figure 6. Putative structures of copper porphyrins detected in the insoluble fraction of the bio-crude based on an attributed molecular formula.

#### 4. Conclusion

Complementarity between EPR and FTICR-MS was highlighted in this work for the characterization of copper porphyrins in an insoluble fraction of a bio-crude. EPR brought to light precious insights about the presence of copper species surrounded by four symmetric nitrogen atoms. FTICR-MS analyses were not precise enough to attribute directly such species. Indeed, the mass difference between copper porphyrins and other molecular formula candidates was too low to avoid misassignments (Figure S2). However, the improved dynamic range afforded by CASI experiments allowed validate the presence of copper porphyrins for the most intense ions and the use of KMD plots to extend the attribution to lower intensity ions. Copper has been already found in bio-crudes [41] but it is the first time, to our knowledge, that it was observed in porphyrins. Such species are extremely resistant, so much that they pass through refining processes and are found in exhaust of motors [15]. Knowing their presence is thus, important for future biofuels design.

#### Acknowledgments

This work has been partially supported by the European Regional Development Fund (ERDF, HN0001343), Labex SynOrg (Grant ANR-11- LABX-0029), Carnot Institute I2C, the Graduate School for Research XL-Chem (Grant ANR-18EURE-0020), the European Union's Horizon 2020 Research Infrastructures program (Grant Agreement 731077), région Normandie, and ADEME for VASCO2 project funding and samples. Access to the CNRS research infrastructure Infranalytics (FR2054) is gratefully acknowledged. Anne Roubaud from CEA LITEN is gratefully acknowledged for her careful reading and editing of the manuscript.

## References

- [1] A. Talec, M. Philistin, F. Ferey, G. Walenta, J.O. Irisson, O. Bernard, A. Sciandra, Effect of gaseous cement industry effluents on four species of microalgae, *Bioresour Technol*, 143 (2013) 353-359. <https://doi.org/10.1016/j.biortech.2013.05.104>
- [2] J.H. Duarte, E.G. de Morais, E.M. Radmann, J.A.V. Costa, Biological CO<sub>2</sub> mitigation from coal power plant by *Chlorella fusca* and *Spirulina* sp, *Bioresour Technol*, 234 (2017) 472-475. <https://doi.org/10.1016/j.biortech.2017.03.066>
- [3] C. Barrère-Mangote, A. Roubaud, B. Bouyssièrre, J. Maillard, J. Hertzog, J.L. Maître, M. Hubert-Roux, J.-F. Sassi, C. Afonso, P. Giusti, Study of Biocrudes Obtained via Hydrothermal Liquefaction (HTL) of Wild Alga Consortium under Different Conditions, *Processes*, 9 (2021) 1494. <https://doi.org/10.3390/pr9091494>
- [4] C. Tian, B. Li, Z. Liu, Y. Zhang, H. Lu, Hydrothermal liquefaction for algal biorefinery: A critical review, *Renewable and Sustainable Energy Reviews*, 38 (2014) 933-950. <https://doi.org/10.1016/j.rser.2014.07.030>
- [5] Y. Guo, T. Yeh, W. Song, D. Xu, S. Wang, A review of bio-oil production from hydrothermal liquefaction of algae, *Renewable and Sustainable Energy Reviews*, 48 (2015) 776-790. <https://doi.org/10.1016/j.rser.2015.04.049>
- [6] S.M. Changi, J.L. Faeth, N. Mo, P.E. Savage, Hydrothermal Reactions of Biomolecules Relevant for Microalgae Liquefaction, *Industrial & Engineering Chemistry Research*, 54 (2015) 11733-11758. <https://doi.org/10.1021/acs.iecr.5c02771>
- [7] S. Chaudry, P.A. Bahri, N.R. Moheimani, Pathways of processing of wet microalgae for liquid fuel production: A critical review, *Renewable and Sustainable Energy Reviews*, 52 (2015) 1240-1250. <https://doi.org/10.1016/j.rser.2015.08.005>
- [8] D. López Barreiro, W. Prins, F. Ronsse, V. Brilman, Hydrothermal liquefaction (HTL) of microalgae for biofuel production: State of the art review and future prospects, *Biomass and Bioenergy*, 53 (2013) 113-127. <https://doi.org/10.1016/j.biombioe.2012.12.029>
- [9] C. Barrère-Mangote, A. Roubaud, B. Bouyssièrre, J. Maillard, J. Hertzog, J.L. Maître, M. Hubert-Roux, J.-F. Sassi, C. Afonso, P.J.P. Giusti, Study of Biocrudes Obtained via Hydrothermal Liquefaction (HTL) of Wild Alga Consortium under Different Conditions, 9 (2021) 1494
- [10] J.M. Jarvis, N.M. Sudasinghe, K.O. Albrecht, A.J. Schmidt, R.T. Hallen, D.B. Anderson, J.M. Billing, T.M. Schaub, Impact of iron porphyrin complexes when hydroprocessing algal HTL biocrude, *Fuel*, 182 (2016) 411-418. <https://doi.org/10.1016/j.fuel.2016.05.107>
- [11] A.G. Marshall, K.P. Rodgers, Petroleomics: chemistry of the underworld, *Proceedings of the National Academy of Sciences of the United States of America*, 105 (2008) 18090-18095. <https://doi.org/10.1073/pnas.0805069105>
- [12] A.G. Marshall, Fourier Transform Ion Cyclotron Resonance Mass Spectrometry, *Acc. Chem. Res.*, 18 (1985) 316-322
- [13] J.F. Maillard, J. Le Maître, C.P. Rüger, M. Ridgeway, C.J. Thompson, B. Paupy, M. Hubert-Roux, M. Park, C. Afonso, P. Giusti, Structural analysis of petroporphyrins from asphaltene by trapped ion mobility coupled with Fourier transform ion cyclotron resonance mass spectrometry, *The Analyst*, 146 (2021) 4161-4171. <https://doi.org/10.1039/d1an00140j>
- [14] B.P. Koch, T. Dittmar, M. Witt, G. Kattner, Fundamentals of molecular formula assignment to ultrahigh resolution mass data of natural organic matter, *Anal Chem*, 79 (2007) 1758-1763. <https://doi.org/10.1021/ac061949s>
- [15] M. Sueur, C.P. Rüger, J.F. Maillard, H. Lavanant, R. Zimmermann, C. Afonso, Selective characterization of petroporphyrins in shipping fuels and their corresponding emissions using electron-transfer matrix-assisted laser desorption/ionization Fourier transform ion cyclotron resonance mass spectrometry, *Fuel*, 332 (2023). <https://doi.org/10.1016/j.fuel.2022.126283>

- [16] J. Ferey, M. Larroque, I. Schmitz-Afonso, J. Le Maitre, O. Sgarbura, S. Carrere, F. Quenet, B. Bouyssiére, C. Enjalbal, S. Mounicou, C. Afonso, Imaging Matrix-Assisted Laser Desorption/Ionization Fourier Transform Ion Cyclotron Resonance Mass Spectrometry of oxaliplatin derivatives in human tissue sections, *Talanta*, 237 (2022) 122915. <https://doi.org/10.1016/j.talanta.2021.122915>
- [17] K. Ben Tayeb, O. Delpoux, J. Barbier, J. Marques, J. Verstraete, H. Vezin, Applications of Pulsed Electron Paramagnetic Resonance Spectroscopy to the Identification of Vanadyl Complexes in Asphaltene Molecules. Part 1: Influence of the Origin of the Feed, *Energy & Fuels*, 29 (2015) 4608-4615. <https://doi.org/10.1021/acs.energyfuels.5b00733>
- [18] A. Abragam, B. Bleaney, *Electron Paramagnetic Resonance of Transition Ions*, 2012.
- [19] A.J. Saraceno, D.T. Fanale, N.D. Coggeshall, An Electron Paramagnetic Resonance Investigation of Vanadium in Petroleum Oils, *Analytical chemistry*, 33 (1961) 500-505. <https://doi.org/10.1021/ac60172a009>
- [20] M.A. Sadovnikova, F.F. Murzakhanov, G.V. Mamin, M.R. Gafurov, HYSORE Spectroscopy to Resolve Electron–Nuclear Structure of Vanadyl Porphyrins in Asphaltenes from the Athabasca Oil Sands In Situ Conditions, *Energies*, 15 (2022). <https://doi.org/10.3390/en15176204>
- [21] J.E. Bruce, G.A. Anderson, H.R. Udseth, R.D. Smith, Large Molecule Characterization Based upon Individual Ion Detection with Electrospray Ionization-FTICR Mass Spectrometry, *Analytical chemistry*, 70 (1998) 519-525. <https://doi.org/10.1021/ac9711706>
- [22] D. Gourier, O. Delpoux, A. Bonduelle, L. Binet, I. Giofini, H. Vezin, EPR, ENDOR, and HYSORE Study of the Structure and the Stability of Vanadyl–Porphyrin Complexes Encapsulated in Silica: Potential Paramagnetic Biomarkers for the Origin of Life, *The Journal of Physical Chemistry B*, 114 (2010) 3714-3723. <https://doi.org/10.1021/jp911728e>
- [23] C. Barrere, M. Hubert-Roux, C.M. Lange, M. Rejaibi, N. Kebir, N. Desilles, L. Lecamp, F. Burel, C. Loutelier-Bourhis, Solvent-based and solvent-free characterization of low solubility and low molecular weight polyamides by mass spectrometry: a complementary approach, *Rapid communications in mass spectrometry : RCM*, 26 (2012) 1347-1354. <https://doi.org/10.1002/rcm.6231>
- [24] J. Peisach, W.E. Blumberg, Structural implications derived from the analysis of electron paramagnetic resonance spectra of natural and artificial copper proteins, *Archives of Biochemistry and Biophysics*, 165 (1974) 691-708. [https://doi.org/10.1016/0003-9861\(74\)90298-7](https://doi.org/10.1016/0003-9861(74)90298-7)
- [25] J.S. Ramirez-Pradilla, C. Blanco-Tirado, M.Y. Combariza, Electron-Transfer Ionization of Nanoparticles, Polymers, Porphyrins, and Fullerenes Using Synthetically Tunable alpha-Cyanophenylenevinylene as UV MALDI-MS Matrices, *ACS Appl Mater Interfaces*, 11 (2019) 10975-10987. <https://doi.org/10.1021/acsami.8b22246>
- [26] J.S. Ramirez-Pradilla, C. Blanco-Tirado, M. Hubert-Roux, P. Giusti, C. Afonso, M.Y. Combariza, Comprehensive Petroporphyrin Identification in Crude Oils Using Highly Selective Electron Transfer Reactions in MALDI-FTICR-MS, *Energy & Fuels*, 33 (2019) 3899-3907. <https://doi.org/10.1021/acs.energyfuels.8b04325>
- [27] J. Maillard, N. Carrasco, I. Schmitz-Afonso, T. Gautier, C. Afonso, Comparison of soluble and insoluble organic matter in analogues of Titan's aerosols, *Earth and Planetary Science Letters*, 495 (2018) 185-191. <https://doi.org/10.1016/j.epsl.2018.05.014>
- [28] R. Tanaka, S. Sato, T. Takanohashi, J.E. Hunt, R.E. Winans, Analysis of the Molecular Weight Distribution of Petroleum Asphaltenes Using Laser Desorption-Mass Spectrometry, *Energy & Fuels*, 18 (2004) 1405-1413. <https://doi.org/10.1021/ef034083r>
- [29] A.G. Marshall, T. Chen, 40 years of Fourier transform ion cyclotron resonance mass spectrometry, *International Journal of Mass Spectrometry*, 377 (2015) 410-420. <https://doi.org/10.1016/j.ijms.2014.06.034>

- [30] C.L. Hendrickson, J.P. Quinn, N.K. Kaiser, D.F. Smith, G.T. Blakney, T. Chen, A.G. Marshall, C.R. Weisbrod, S.C. Beu, 21 Tesla Fourier Transform Ion Cyclotron Resonance Mass Spectrometer: A National Resource for Ultrahigh Resolution Mass Analysis, *Journal of the American Society for Mass Spectrometry*, 26 (2015) 1626-1632.<https://doi.org/10.1007/s13361-015-1182-2>
- [31] L.C. Krajewski, R.P. Rodgers, A.G. Marshall, 126 264 Assigned Chemical Formulas from an Atmospheric Pressure Photoionization 9.4 T Fourier Transform Positive Ion Cyclotron Resonance Mass Spectrum, *Analytical chemistry*, 89 (2017) 11318-11324.<https://doi.org/10.1021/acs.analchem.7b02004>
- [32] C.J. Thompson, M. Witt, S. Forcisi, F. Moritz, N. Kessler, F.H. Laukien, P. Schmitt-Kopplin, An Enhanced Isotopic Fine Structure Method for Exact Mass Analysis in Discovery Metabolomics: FIA-CASI-FTMS, *Journal of the American Society for Mass Spectrometry*, 31 (2020) 2025-2034.<https://doi.org/10.1021/jasms.0c00047>
- [33] E.N. Nikolaev, Y.I. Kostyukevich, G.N. Vladimirov, Fourier transform ion cyclotron resonance (FT ICR) mass spectrometry: Theory and simulation, *Mass Spectrom Rev*, 35 (2016) 219-258.<https://doi.org/10.1002/mas.21422>
- [34] J.M. Jarvis, N.M. Sudasinghe, K.O. Albrecht, A.J. Schmidt, R.T. Hallen, D.B. Anderson, J.M. Billing, T.M.J.F. Schaub, Impact of iron porphyrin complexes when hydroprocessing algal HTL biocrude, 182 (2016) 411-418
- [35] F. Zheng, C.S. Hsu, Y. Zhang, Y. Sun, Y. Wu, H. Lu, X. Sun, Q.J.E. Shi, *Fuels*, Simultaneous detection of vanadyl, nickel, iron, and gallium porphyrins in marine shales from the Eagle Ford Formation, South Texas, 32 (2015) 10382-10390
- [36] E. Kendrick, A Mass Scale Based on  $^{12}\text{C} = 14.0000$  for High Resolution Mass Spectrometry of Organic Compounds, *Analytical chemistry*, 35 (1963) 2146-2154.<https://doi.org/10.1021/ac60206a048>
- [37] C.A. Hughey, C.L. Hendrickson, R.P. Rodgers, A.G. Marshall, K. Qian, Kendrick Mass Defect Spectrum: A Compact Visual Analysis for Ultrahigh-Resolution Broadband Mass Spectra, *Analytical chemistry*, 73 (2001) 4676-4681.<https://doi.org/10.1021/ac010560w>
- [38] M. Sueur, J.F. Maillard, O. Jacquot-Andrivet, C.P. Rüger, P. Giusti, H. Lavanant, C. Afonso, PyC2MC: an open-source software solution for visualization and treatment of high-resolution mass spectrometry data, *Analytical Chemistry*, (2022).<https://doi.org/10.26434/chemrxiv-2022-cmnk3>
- [39] F. Zheng, Y. Zhang, Y. Zhang, Y. Han, L. Zhang, B. Bouyssiere, Q. Shi, Aggregation of petroporphyrins and fragmentation of porphyrin ions: Characterized by TIMS-TOF MS and FT-ICR MS, *Fuel*, 289 (2021).<https://doi.org/10.1016/j.fuel.2020.119889>
- [40] A.M. McKenna, M.J. Chacón-Patiño, G. Salvato Vallverdu, B. Bouyssiere, P. Giusti, C. Afonso, Q. Shi, M.Y. Combariza, Advances and Challenges in the Molecular Characterization of Petroporphyrins, *Energy & Fuels*, (2021).<https://doi.org/10.1021/acs.energyfuels.1c02002>
- [41] J. Jiang, P.E.J.E. Savage, *Fuels*, Metals and other elements in biocrude from fast and isothermal hydrothermal liquefaction of microalgae, 32 (2017) 4118-4126



Author Statement

Julien F. Maillard: Methodology, Validation, Investigation, Resources, Data curation, Writing – original draft, Writing – review & editing, Visualization.

Charlotte Mase: Methodology, Validation, Investigation, Resources, Data curation, Writing – original draft, Writing – review & editing, Visualization.

Olivier Serve: Conceptualization, Methodology, Writing – review & editing

Hervé Vezin: Conceptualization, Methodology, Writing – review & editing, Data curation

Carlos Afonso: Conceptualization, Methodology, Writing – review & editing, Supervision, Project administration, Funding acquisition.

Pierre Giusti: Conceptualization, Writing – review & editing, Supervision, Supervision, Funding acquisition.

Caroline Mangote: Conceptualization, Writing – review & editing, Supervision, Supervision, Funding acquisition.

**Declaration of interests**

The authors declare that they have no known competing financial interests or personal relationships that could have appeared to influence the work reported in this paper.

The authors declare the following financial interests/personal relationships which may be considered as potential competing interests:

Journal Pre-proof



**Highlights**

- First identification of copper-porphyrins in bio-crudes
- Complementarity between EPR and FTICR-MS for copper-porphyrins speciation
- EPR brought precious insights about the environment of copper atoms
- Kendrick mass defect plots to extend the attribution of lower intensity ions

Journal Pre-proof